COMMUN. MATH. SCI.
Vol. 16, No. 4, pp. 1131–1154

BLOWUP FROM RANDOMLY SWITCHING BETWEEN STABLE BOUNDARY CONDITIONS FOR THE HEAT EQUATION*

SEAN D. LAWLEY†

Abstract. We find a pair of boundary conditions for the heat equation such that the solution goes to zero for either boundary condition, but if the boundary condition randomly switches, then the average solution grows exponentially in time. Specifically, we prove that the mean of the random solution grows exponentially under certain mild assumptions, and we use formal asymptotic methods to argue that the random solution grows exponentially almost surely. To our knowledge, this could be the first PDE example showing that randomly switching between two globally asymptotically stable systems can produce a blowup. We devise several methods to analyze this random PDE. First, we use the method of lines to approximate the switching PDE by a large number of switching ODEs and then apply recent results to determine if they grow or decay in the limit of fast switching. We then use perturbation theory to obtain more detailed information on the switching PDE in this fast switching limit. To understand the case of finite switching rates, we characterize the parameter regimes in which the first and second moments of the random PDE grow or decay. This moment analysis reveals rich dynamical behavior, including a region of parameter space in which the mean of the random PDE oscillates with ever increasing amplitude for slow switching rates, grows exponentially for fast switching rates, but decays to zero for intermediate switching rates. We also highlight cases in which the second moment is necessary to understand the switching system's qualitative behavior, rather than just the mean. Finally, we give a PDE example in which randomly switching between two unstable systems produces a stable system. All of our analysis is accompanied by numerical simulation.

Keywords. piecewise deterministic Markov process; switched dynamical systems; stochastic hybrid system; random PDE; thermostat model.

AMS subject classifications. 35R60; 60H15; 93E15; 35K05; 35B44.

1. Introduction

Randomly switching dynamical systems have generated much interest in the probability literature recently [2–4, 7–9, 21, 29, 30, 48] and are involved in a growing number of applications to biology [11, 12, 20, 52], physics [6, 18], engineering [25, 31, 53], and finance [57]. Due to the diversity of the groups studying these switching systems, they have been given several names, including stochastic hybrid systems, piecewise deterministic Markov processes, dichotomous Markov noise processes, velocity jump processes, and random evolutions.

Such a switching system can be described by a continuous component $\{U(t)\}_{t\geq 0}$ and a discrete component $\{J(t)\}_{t\geq 0}$. The discrete component J is a jump process, and for each element of its state space we assign some continuous dynamics to U. In between jumps of J, the component U evolves according to the dynamics associated with the current state of J. When J jumps, U switches to following the dynamics associated with the new state of J. Typically, one assumes that U takes values in $\mathbb{R}^d$ and is driven by an ordinary differential equation (ODE) in between jumps of J,

$$\tfrac{d}{dt}U(t) = F_{J(t)}\big(U(t)\big) \in \mathbb{R}^d, \tag{1.1}$$

where $\{F_j(u)\}_j$ are a given set of vector fields.

Benaim et al. [8] have recently demonstrated that systems of the form (1.1) can exhibit surprising qualitative behavior (see also [10, 40, 44, 49]). Specifically, they showed

*Received: August 18, 2017; Accepted (in revised form): April 3, 2018. Communicated by David Anderson.

†Department of Mathematics, University of Utah, Salt Lake City, UT 84112 USA (lawley@math.utah.edu).

that a planar process $U(t)\in\mathbb{R}^2$ driven by a pair of linear ODEs,

$$\tfrac{d}{dt}U(t)=A_{J(t)}U(t), \tag{1.2}$$

with $A_0,A_1\in\mathbb{R}^{2\times 2}$, $J(t)\in\{0,1\}$ can blowup,

$$\|U(t)\|\to\infty \quad \text{almost surely as } t\to\infty,$$

even if all the eigenvalues of both matrices A_0 and A_1 have strictly negative real part. That is, the individual systems $\frac{d}{dt}U=A_0U$ and $\frac{d}{dt}U=A_1U$ decay to zero, but the switched system (1.2) grows without bound. A key to the proof in [8] is writing (1.2) in polar coordinates and determining the behavior of the radial coordinate from the invariant measure of the angular coordinate.

In this paper, we analyze a randomly switching partial differential equation (PDE) whose qualitative behavior is similar in spirit to the ODE systems in [8]. Specifically, we find a pair of boundary conditions (BCs) for the heat equation such that the solution goes to zero for either BC, but if the BC randomly switches, then the average solution grows exponentially in time. In particular, we prove that the mean of the random solution grows exponentially under certain mild assumptions, and we use formal asymptotic methods to argue that the random solution grows exponentially almost surely. To our knowledge, this could be the first PDE example showing that randomly switching between two globally asymptotically stable systems can produce a blowup. This system is motivated by recent biological models involving the diffusion equation with randomly switching boundary conditions [14–16, 42, 43, 45].

In order to analyze this random PDE, we employ a variety of methods. First, we use the method of lines to discretize space and approximate the switching PDE by a large number of switching ODEs. We then use recent results to determine if these switching ODEs grow or decay in the limit of fast switching. Next, we use perturbation theory to obtain more detailed information on the switching PDE in this fast switching limit. In particular, this perturbation argument shows that the PDE converges formally for fast switching to a deterministic PDE which we solve explicitly. To understand the case of finite switching rates, we characterize the parameter regimes in which the first and second moments of the random PDE grow or decay. This moment analysis reveals rich dynamical behavior, including a region of parameter space in which the mean of the random PDE oscillates with ever increasing amplitude for slow switching rates, grows exponentially for fast switching rates, but decays to zero for intermediate switching rates. We also highlight cases in which the second moment is necessary to understand the switching system's qualitative behavior, rather than just the mean. Throughout the paper, we compare our analytical results to numerical simulations.

The paper is organized as follows. In Section 2, we setup our randomly switching PDE. In Section 3, we analyze the random PDE in the limit of fast switching. In Section 4, we analyze the first and second moments of the random PDE for finite switching rates. In Section 5, we give a PDE example in which randomly switching between two unstable systems produces a stable system. We note that the average system for this final example is stable. We conclude with a brief discussion.

2. Problem setup

The following PDE boundary value problem is the so-called *thermostat model*,

$$\begin{aligned} \tfrac{\partial}{\partial t}u&=\tfrac{\partial^2}{\partial x^2}u, \quad x\in(0,1),t>0,\\ \tfrac{\partial}{\partial x}u(0,t)&=\gamma u(1,t), \qquad \tfrac{\partial}{\partial x}u(1,t)=0, \end{aligned} \tag{2.1}$$

with parameter $\gamma > 0$, which models the temperature $u(x,t)$ in a one-dimensional corridor $[0,1]$. First proposed by Guidotti and Merino [27, 28], this model has been well-studied due to its rich behavior [19, 23, 32–34, 36–38, 50, 51, 54–56]. The key feature of this model is the nonlocal BC in which the amount of heating at $x=0$ depends on the temperature at $x=1$. This models the generic situation in which a heating unit and its temperature sensor are at different locations. It is known that a Hopf bifurcation from the trivial solution occurs at a critical parameter value $\gamma_c > 0$ [27, 36]. Indeed, if $\gamma < \gamma_c$, then solutions decay to zero, but if $\gamma > \gamma_c$, then solutions oscillate with ever increasing amplitude. Reference [27] determined that (see also [36])

$$\gamma_c \approx 17.8. \tag{2.2}$$

Note that swapping the locations of the heater and the sensor yields

$$\begin{aligned} \tfrac{\partial}{\partial t}u = \tfrac{\partial^2}{\partial x^2}u, \quad x \in (0,1), t > 0, \\ \tfrac{\partial}{\partial x}u(0,t) = 0, \qquad \tfrac{\partial}{\partial x}u(1,t) = -\gamma u(0,t). \end{aligned} \tag{2.3}$$

In this paper, we analyze the following randomly switching thermostat model,

$$\begin{aligned} \tfrac{\partial}{\partial t}u = \tfrac{\partial^2}{\partial x^2}u, \quad x \in (0,1), t > 0, \\ \tfrac{\partial}{\partial x}u(0,t) = (1-J(t))\gamma u(1,t), \qquad \tfrac{\partial}{\partial x}u(1,t) = -J(t)\gamma u(0,t), \end{aligned} \tag{2.4}$$

where $J(t) \in \{0,1\}$ is a two-state Markov jump process with jump rate $\alpha > 0$,

$$0 \underset{\alpha}{\overset{\alpha}{\rightleftharpoons}} 1. \tag{2.5}$$

When $J(t) = 0$, (2.4) reduces to (2.1), and when $J(t) = 1$, (2.4) reduces to (2.3). Hence, (2.4) corresponds to repeatedly swapping the locations of the heater and the sensor. We note that (2.4) was mentioned briefly in our previous work [41] in order to motivate the general theorems proved therein.

We will seek to choose $\gamma < \gamma_c$ so that the randomly switching system (2.4) grows without bound, even though the two individual non-switched systems ((2.1) and (2.3)) decay to zero for this choice of γ.

We conclude this section by constructing the random solution to (2.4). Let

$$\exp(\mathbb{A}_0 t) : L^2[0,1] \to L^2[0,1]$$

denote the solution operator of (2.1). That is, $\exp(\mathbb{A}_0 t)$ takes an initial condition and maps it to the solution of (2.1) at time $t \geq 0$. Similarly, let $\exp(\mathbb{A}_1 t)$ denote the solution operator of (2.3). These operators are analytic C_0-semigroups [28]. Random solutions of (2.4) are constructed by repeatedly composing $\exp(\mathbb{A}_0 t)$ and $\exp(\mathbb{A}_1 t)$ according to the jumps of J. Let $\{\xi_k\}_{k=1}^{\infty}$ denote the sequence of states visited by J, and $\{s_k\}_{k=1}^{\infty}$ be the sojourn times in each state. That is, let $\xi_1 \in \{0,1\}$ be a Bernoulli random variable with mean $1/2$ and let $\xi_k = 1 - \xi_{k\pm 1}$ and $J(t) = \xi_k$ if

$$t \in \Big[\sum_{j=1}^{k-1} s_j, \sum_{j=1}^{k} s_j\Big),$$

where $\{s_k\}_{k=1}^{\infty}$ is a sequence of independent exponential random variables, each with rate $\alpha > 0$. Let $N(t)$ be the number of jumps of J before time t,

$$N(t) := \sup\Big\{k \in \mathbb{N} \cup \{0\} : \sum_{j=1}^{k} s_j < t\Big\},$$

and let $a(t) := t - \sum_{j=1}^{N(t)} s_j$ be the time since the last jump (often called the "age" process in renewal theory). Then the solution to (2.4) at time $t \geq 0$ is

$$u(x,t) = \exp(\mathbb{A}_{\xi_{N(t)+1}} a(t)) \exp(\mathbb{A}_{\xi_{N(t)}} s_{N(t)}) \cdots \exp(\mathbb{A}_{\xi_1} s_1) u(x,0). \tag{2.6}$$

3. Fast switching

In this section, we investigate (2.4) in the fast switching limit ($\alpha \gg 1$). Our analysis predicts that the critical value of γ for the switched system in this limit is

$$\gamma_c^{\mathrm{sw}} = 4 < \gamma_c \approx 17.8.$$

That is, if $\gamma \in (4, \gamma_c)$, then the switched system (2.4) grows without bound for sufficiently fast switching, whereas the two individual systems ((2.1) and (2.3)) decay to zero.

3.1. Method of lines. We begin by using the method of lines [46] to approximate the randomly switching PDE (2.4) by a randomly switching ODE. We then use recent results [44] to analyze this randomly switching ODE in the limit of fast switching. In addition, the switching ODE that we derive here will continue to inform our study of the switching PDE (2.4) in later sections.

To derive the approximating ODEs, ignore the switching for the moment and consider the deterministic PDE (2.1). Introduce a spatial discretization $\Delta x = 1/N$ for $N \in \mathbb{N}$ and evaluate the solution $u(x,t)$ at grid points to form $N+1$ functions of time

$$u_i(t) := u(i\Delta x, t), \quad i = 0, 1, \ldots, N.$$

Discretizing the Laplacian operator in (2.1), we have the following ODE at interior grid points,

$$\tfrac{d}{dt} u_i(t) = N^2 \big[u_{i+1}(t) - 2u_i(t) + u_{i-1}(t)\big] + \mathcal{O}(N^{-2}), \quad i = 1, \ldots, N-1. \tag{3.1}$$

To implement the BCs in (2.1), we first introduce so-called ghost points [17],

$$u_{-1}(t) := u(-\Delta x, t), \quad u_{N+1}(t) := u(1 + \Delta x, t),$$

by extending $u(x,t)$ to $x \in (-1, 2)$ according to

$$u(-x,t) = -u(x,t) + 2u(0,t), \quad u(1+x,t) = u(1-x,t), \quad x \in (0,1).$$

It follows that (3.1) is satisfied at $i = 0$ and $i = N$. Since the BCs in (2.1) are satisfied by the extension to $(-1, 2)$, we have that

$$\begin{aligned} \tfrac{\partial}{\partial x} u(0,t) &= (N/2)\big[u_1(t) - u_{-1}(t)\big] + \mathcal{O}(N^{-2}) = \gamma u_N(t) \\ \tfrac{\partial}{\partial x} u(1,t) &= (N/2)\big[u_{N+1}(t) - u_{N-1}(t)\big] + \mathcal{O}(N^{-2}) = 0. \end{aligned} \tag{3.2}$$

Combining (3.2) with (3.1) to eliminate the ghost points, we have that

$$\begin{aligned} \tfrac{d}{dt} u_0(t) &= N^2\big[2u_1(t) - 2u_0(t) - 2(\gamma/N) u_N(t)\big] + \mathcal{O}(N^{-2}), \\ \tfrac{d}{dt} u_N(t) &= N^2\big[2u_N(t) - 2u_{N-1}(t)\big] + \mathcal{O}(N^{-2}). \end{aligned} \tag{3.3}$$

Putting (3.1) and (3.3) in vector notation and dropping the $\mathcal{O}(N^{-2})$, we approximate the solution to (2.1) by the ODE

$$\tfrac{d}{dt} U_N(t) = A_0 U_N(t), \tag{3.4}$$

where

$$U_N(t) = (u_0(t), u_1(t), \ldots, u_N(t)) \in \mathbb{R}^{N+1},$$

and $A_0 \in \mathbb{R}^{(N+1)\times(N+1)}$ is the matrix

$$A_0 = N^2 \begin{pmatrix} -2 & 2 & & & -2\gamma/N \\ 1 & -2 & 1 & & \\ & \ddots & \ddots & \ddots & \\ & & 1 & -2 & 1 \\ & & & 2 & -2 \end{pmatrix}. \tag{3.5}$$

Analogously, we approximate the solution to (2.3) by

$$\tfrac{d}{dt} U_N(t) = A_1 U_N(t), \tag{3.6}$$

where A_1 is given by A_0 after swapping the last entry in the first row with the first entry in the last row.

The derivation of (3.4) and (3.6) is the standard numerical method known as the method of lines [46], which approximates a PDE by a large number of ODEs. Assuming the ODEs (3.4) and (3.6) are good approximations of the corresponding PDEs (2.1) and (2.3), it follows that we can approximate the randomly switching PDE (2.4) by a randomly switching ODE. We make this precise in the following proposition.

PROPOSITION 3.1. *For $N \in \mathbb{N}$, let $D_N : L^2[0,1] \to \mathbb{R}^{N+1}$ denote the discretization operator that maps a function to the vector obtained from evaluating the function at grid points,*

$$D_N(f) := (f(0), f(1/N), \ldots, f(1)) \in \mathbb{R}^{N+1}.$$

Let $u(x,t)$ be the solution to the randomly switching PDE (2.4) and suppose $U_N(t) \in \mathbb{R}^{N+1}$ satisfies the randomly switching ODE

$$\tfrac{d}{dt} U_N(t) = A_{J(t)} U_N(t), \tag{3.7}$$

with initial condition $U_N(0) = D_N(u(x,0))$. Assume that for each $f \in L^2[0,1]$, $t > 0$, and $j \in \{0,1\}$, we have that

$$\|\exp(A_j t) D_N(f) - D_N(\exp(\mathbb{A}_j t) f)\| \to 0, \quad \text{as } N \to \infty. \tag{3.8}$$

Further, assume that for each $t > 0$, there exists a constant $\kappa(t)$ such that for all $N \in \mathbb{N}$ and $j \in \{0,1\}$, we have that

$$\|\exp(A_j t)\| \le \kappa(t). \tag{3.9}$$

Then

$$\|U_N(T) - D_N(u(x,T))\| \to 0 \quad \text{almost surely as } N \to \infty. \tag{3.10}$$

Proof. Fix $T \ge 0$. To show the almost sure convergence in (3.10), fix a realization of the jump process $\{J(t)\}_{t\ge 0}$. For this realization of J, there exists a finite sequence of positive times $\{\tau_k\}_{k=1}^K$ and a finite sequence $\{\xi_k\}_{k=1}^K$ with $\xi_k \in \{0,1\}$ such that

$$\begin{aligned} u(x,T) &= \exp(\mathbb{A}_{\xi_K}\tau_K)\exp(\mathbb{A}_{\xi_{K-1}}\tau_{K-1})\cdots\exp(\mathbb{A}_{\xi_1}\tau_1) f \in L^2[0,1], \\ U_N(T) &= \exp(A_{\xi_K}\tau_K)\exp(A_{\xi_{K-1}}\tau_{K-1})\cdots\exp(A_{\xi_1}\tau_1) D_N f \in \mathbb{R}^{N+1}, \end{aligned} \tag{3.11}$$

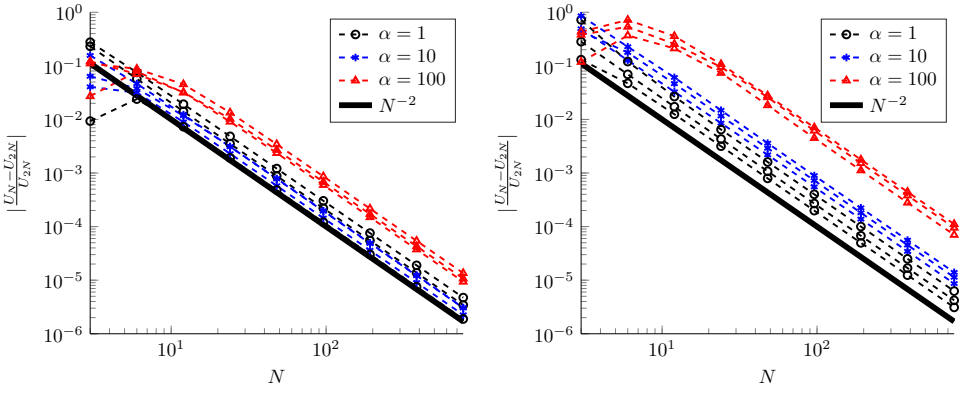

FIG. 3.1. *The error in approximating (2.4) by (3.7) decays like N^{-2} as N grows. Both panels plot the relative error, $|U_N - U_{2N}|/|U_{2N}|$, as a function of the spatial discretization, N. Each dashed curve corresponds to a particular stochastic realization of the jump process, J. The vectors U_N, U_{2N} are evaluated at their first entry at $t=1$. We set $\gamma=3$ in the left plot and set $\gamma=5$ in the right plot.*

where $f(x) := u(x,0)$.

Using the representations in (3.11), the proof proceeds by induction on $K \geq 1$. The base case $K=1$ holds by assumption. For $K>1$, observe that

$$\begin{aligned}
&\|U_N(T) - D_N(u(x,T))\| \\
\leq &\|U_N(T) - \exp(A_{\xi_K}\tau_K) D_N \exp(\mathbb{A}_{\xi_{K-1}}\tau_{K-1}) \cdots \exp(\mathbb{A}_{\xi_1}\tau_1) f\| \\
&\quad + \|\exp(A_{\xi_K}\tau_K) D_N \exp(\mathbb{A}_{\xi_{K-1}}\tau_{K-1}) \cdots \exp(\mathbb{A}_{\xi_1}\tau_1) f - D_N(u(x,T))\| \\
\leq &M \|\exp(A_{\xi_K}\tau_K)\| + \|\exp(A_{\xi_K}\tau_K) D_N g - D_N \exp(\mathbb{A}_{\xi_K}\tau_K) g\|,
\end{aligned}$$

where

$$\begin{aligned}
M &:= \|\exp(A_{\xi_{K-1}}\tau_{K-1}) \cdots \exp(A_{\xi_1}\tau_1) D_N f - D_N \exp(\mathbb{A}_{\xi_{K-1}}\tau_{K-1}) \cdots \exp(\mathbb{A}_{\xi_1}\tau_1) f\|, \\
g &:= \exp(\mathbb{A}_{\xi_{K-1}}\tau_{K-1}) \cdots \exp(\mathbb{A}_{\xi_1}\tau_1) f.
\end{aligned}$$

Using (3.9), the inductive hypothesis and (3.8) the proof is complete. ∎

While we do not rigorously verify the hypotheses (Equations (3.8) and (3.9)) of Proposition 3.1, extensive numerical tests suggest that they hold. Furthermore, Figure 3.1 suggests that the error in approximating (2.4) by (3.7) decays like N^{-2} as N grows. In light of this, we proceed with studying the randomly switching ODE (3.7) in the remainder of this subsection. We will find that the result of our analysis (the critical value of γ in Theorem 3.1) agrees with both (a) the limiting PDE derived from perturbation theory in Section 3.2, and (b) the analysis of the mean PDE in Section 4 (see (4.18)). We note that the mean PDE analysis in Section 4 is independent of the ODE approximation in the present section.

In general, the behavior of switching linear ODEs such as (3.7) can depend on the switching rate $\alpha > 0$ in an extremely complicated way [44]. However, it is known that for fast switching ($\alpha \gg 1$), the behavior is determined by the spectrum of the average matrix, $A := \frac{1}{2}(A_0 + A_1)$ [22, 44]. The following proposition investigates the spectrum of A as a function of the parameter $\gamma > 0$. For simplicity, we henceforth assume that N is odd.

PROPOSITION 3.2. *If $\gamma<4$, then all the eigenvalues of A are strictly negative. If $\gamma>4$, then A has a strictly positive eigenvalue.*

Proof. We seek the eigenvalues $\{\lambda_k\}_{k=0}^N$ of the matrix $B:=1/N^2A+2I$ since the eigenvalues of A are then given by

$$\{N^2(\lambda_k-2)\}_{k=0}^N. \tag{3.12}$$

Writing $B\mathbf{v}=\lambda\mathbf{v}$ component wise, we have

$$v_{k-1}+v_{k+1}=\lambda v_k, \quad k=1,\dots,N, \tag{3.13}$$
$$2v_1-\Delta x\gamma v_N=\lambda v_0, \tag{3.14}$$
$$2v_{N-1}-\Delta x\gamma v_0=\lambda v_N. \tag{3.15}$$

If $\lambda=2\cos(\varphi)$ for $\varphi\in\mathbb{C}$ and $v_k=\cos(\theta+k\varphi)$, then (3.13) is satisfied by an elementary trigonometric identity. Letting $\theta=-\varphi N/2$ makes (3.14) and (3.15) into the same equation, which after some manipulation is

$$2N\tan(\varphi N/2)\sin(\varphi)=\gamma. \tag{3.16}$$

Since $\tan(yN/2)$ has $\lfloor N/2\rfloor$-many points $y_0\in(0,\pi)$ such that $\lim_{y\to y_0\mp}\tan(N/2y)=\pm\infty$, it is easy to see that (3.16) has at least $\lfloor N/2\rfloor$-many solutions $\varphi\in(0,\pi)$.

Further, observe that

$$\lim_{\varphi\to\pi}2N\tan(\varphi N/2)\sin(\varphi)=4.$$

Hence, if $\gamma<4$, then there is an additional solution $\varphi\in(0,\pi)$ to (3.16) yielding a total of $\lceil N/2\rceil$-many real solutions to (3.16). Furthermore, it is easy to see from (3.13)-(3.15) that if $(\lambda,\mathbf{v})$ is an eigenpair, then $(-\lambda,\mathbf{v}')$ is also an eigenpair with

$$v_k':=(-1)^kv_k.$$

Hence if $\gamma<4$, then we have found the $N+1$ eigenvalues of B, each of the form $\lambda=\pm2\cos(\varphi)$ with $\varphi\in\mathbb{R}$. Since the eigenvalues of A are then given by (3.12), it follows that all the eigenvalues of A are strictly negative.

On the other hand, if $\gamma>4$, then there is a complex solution to (3.16) given by

$$\varphi=\pi+bi\in\mathbb{C},$$

where $b\in\mathbb{R}\backslash\{0\}$ satisfies

$$2N\coth(bN/2)\sinh(b)=\gamma.$$

Hence, there is an eigenvalue of B given by $\lambda=2\cos(\pi+bi)=2\cosh(b)>2$ and thus A has a positive eigenvalue by (3.12). ∎

Having characterized the spectrum of the average matrix A, we now determine the behavior of (3.7) for fast switching ($\alpha\gg1$).

THEOREM 3.1. *If $\gamma<4$, then there exists an $\alpha_c>0$ such that if $\alpha>\alpha_c$, then*

$$\|U_N(t)\|\to0 \quad \textit{almost surely as } t\to\infty.$$

If $\gamma > 4$, then $\|\exp(At)\| \to \infty$ as $t \to \infty$, and for each $t > 0$ we have that

$$\|U_N(t) - \exp(At) D_N(u(x,0))\| \to 0 \quad \text{in probability as } \alpha \to \infty. \tag{3.17}$$

Proof. By Proposition 3.2, if $\gamma < 4$, then all the eigenvalues of A are strictly negative. Hence, the first assertion of the theorem follows directly from Theorem 2.4 of [44].

Next, assume $\gamma > 4$. By Proposition 3.2, A has a strictly positive eigenvalue and thus $\|\exp(At)\| \to \infty$ as $t \to \infty$. To show the convergence in (3.17), we need some more notation. Recalling $\{\xi_k\}_{k=1}^{\infty}$, $\{s_k\}_{k=1}^{\infty}$, $\{N(t)\}_{t\geq 0}$, and $\{a(t)\}_{t\geq 0}$ introduced in Section 2, define the solution operator for (3.7),

$$S(t) := \exp(A_{\xi_{N(t)+1}} a(t)) \exp(A_{\xi_{N(t)}} s_{N(t)}) \cdots \exp(A_{\xi_1} s_1).$$

Next, let $\{J^{(1)}(t)\}_{t\geq 0}$ be a Markov process on $\{0,1\}$ with switching rate 1 and define $\{\xi_k^{(1)}\}_{k=1}^{\infty}$, $\{s_k^{(1)}\}_{k=1}^{\infty}$, $\{N^{(1)}(t)\}_{t\geq 0}$, and $\{a^{(1)}(t)\}_{t\geq 0}$ as in Section 2 but now with respect to $\{J^{(1)}(t)\}_{t\geq 0}$. For each $\alpha > 0$, define the operator

$$\widetilde{S}^{(\alpha)}(t) := \exp\left(A_{\xi_1^{(1)}} \frac{s_1^{(1)}}{\alpha}\right) \cdots \exp\left(A_{\xi_{N^{(1)}(\alpha t)}} \frac{s_{N^{(1)}(\alpha t)}^{(1)}}{\alpha}\right) \exp\left(A_{\xi_{N^{(1)}(\alpha t)+1}} \frac{a^{(1)}(\alpha t)}{\alpha}\right).$$

By construction, $\widetilde{S}^{(\alpha)}(t)$ and $S(t)$ are equal in distribution.

Applying Theorem 2.1 of [39], we have that $\widetilde{S}^{(\alpha)}(t) \to \exp(At)$ almost surely in the strong operator topology as $\alpha \to \infty$. Since $\mathbb{R}^{N+1}$ is finite-dimensional, the convergence actually holds in the uniform operator topology. That is,

$$\|\widetilde{S}^{(\alpha)}(t) - \exp(At)\| \to 0 \quad \text{almost surely as } \alpha \to \infty.$$

Since almost sure convergence implies convergence in probability, and since $\widetilde{S}^{(\alpha)}(t)$ and $S(t)$ are equal in distribution, the proof is complete. ∎

3.2. Limiting PDE. The analysis in the previous subsection allowed us to prove that discretized approximations to (2.4) either decay to zero or grow without bound in the limit of fast switching, depending if the parameter γ is less than or greater than 4. However, we have not proven that the actual PDE (2.4) exhibits this behavior. In this subsection, we use perturbation theory to argue formally that the PDE (2.4) does indeed exhibit this behavior. Furthermore, our perturbation argument yields more detailed information on the behavior of the PDE (2.4) in this fast switching limit.

As above, suppose $U_N(t)$ satisfies (3.7) and denote its probability density by

$$p_j(\mathbf{u},t)\, d\mathbf{u} = \mathbb{P}(U_N(t) \in (\mathbf{u}, \mathbf{u}+d\mathbf{u}) \cap J(t) = j), \quad j \in \{0,1\}, \mathbf{u} \in \mathbb{R}^{N+1}. \tag{3.18}$$

Assuming the density exists, it evolves according to the forward differential Chapman-Kolmogorov equation [24]

$$\frac{\partial}{\partial t} p_j(\mathbf{u},t) = -\nabla \cdot ((A_j \mathbf{u}) p_j(\mathbf{u},t)) + \alpha(p_{1-j}(\mathbf{u},t) - p_j(\mathbf{u},t)), \quad j = 0,1. \tag{3.19}$$

Let $\varepsilon = 1/\alpha \ll 1$ and introduce the following asymptotic expansion for p_j,

$$\begin{pmatrix} p_0(\mathbf{v},t) \\ p_1(\mathbf{v},t) \end{pmatrix} = \begin{pmatrix} p_0^{(0)}(\mathbf{v},t) \\ p_1^{(0)}(\mathbf{v},t) \end{pmatrix} + \varepsilon \begin{pmatrix} p_0^{(1)}(\mathbf{v},t) \\ p_1^{(1)}(\mathbf{v},t) \end{pmatrix} + \varepsilon^2 \begin{pmatrix} p_0^{(2)}(\mathbf{v},t) \\ p_1^{(2)}(\mathbf{v},t) \end{pmatrix} + \ldots. \tag{3.20}$$

If W denotes the matrix

$$W := \begin{pmatrix} -1 & 1 \\ 1 & -1 \end{pmatrix}, \tag{3.21}$$

then plugging the expansion (3.20) into (3.19) yields the $\mathcal{O}(1/\varepsilon)$ equation

$$W \begin{pmatrix} p_0^{(0)}(\mathbf{v},t) \\ p_1^{(0)}(\mathbf{v},t) \end{pmatrix} = 0, \tag{3.22}$$

and the $\mathcal{O}(1)$ equation

$$W \begin{pmatrix} p_0^{(1)}(\mathbf{v},t) \\ p_1^{(1)}(\mathbf{v},t) \end{pmatrix} = \frac{\partial}{\partial t} \begin{pmatrix} p_0^{(0)}(\mathbf{v},t) \\ p_1^{(0)}(\mathbf{v},t) \end{pmatrix} + \begin{pmatrix} \nabla \cdot \big((A_0 \mathbf{v}) p_0^{(0)}(\mathbf{v},t) \big) \\ \nabla \cdot \big((A_1 \mathbf{v}) p_1^{(0)}(\mathbf{v},t) \big) \end{pmatrix}. \tag{3.23}$$

Equation (3.22) implies that $p_0^{(0)} = p_1^{(0)} =: p^{(0)}$. In order for (3.23) to be solvable, the Fredholm alternative stipulates that the righthand side of (3.23) must be orthogonal to the nullspace of the transpose of W. Hence,

$$\tfrac{\partial}{\partial t} p^{(0)}(\mathbf{v},t) + \nabla \cdot \big((A_0 \mathbf{v}) p^{(0)}(\mathbf{v},t) \big) = -\Big\{ \tfrac{\partial}{\partial t} p^{(0)}(\mathbf{v},t) + \nabla \cdot \big((A_1 \mathbf{v}) p^{(0)}(\mathbf{v},t) \big) \Big\}. \tag{3.24}$$

Rearranging (3.24), we find that $p^{(0)}$ satisfies the Liouville equation

$$\tfrac{\partial}{\partial t} p^{(0)}(\mathbf{v},t) = -\nabla \cdot \big((A \mathbf{v}) p^{(0)}(\mathbf{v},t) \big),$$

with $A := \frac{1}{2}(A_0 + A_1)$. Assuming deterministic initial conditions, the Liouville equation is equivalent to the deterministic ODE

$$\tfrac{d}{dt} \overline{U}_N(t) = A \overline{U}_N(t).$$

Observing the structure of A and retaking the continuum limit $N \to \infty$ implies that the random solution $u(x,t)$ to (2.4) converges formally in the fast switching limit to a deterministic function $\overline{u}(x,t)$ which satisfies

$$\begin{aligned} &\tfrac{\partial}{\partial t} \overline{u} = \tfrac{\partial^2}{\partial x^2} \overline{u}, \quad x \in (0,1), t > 0, \\ &\tfrac{\partial}{\partial x} \overline{u}(0,t) = (\gamma/2) \overline{u}(1,t), \qquad \tfrac{\partial}{\partial x} \overline{u}(1,t) = -(\gamma/2) \overline{u}(0,t). \end{aligned} \tag{3.25}$$

As one might expect, these BCs are the BCs obtained by replacing $J(t)$ by its average $1/2$ in (2.4).

Under some technical assumptions, we can also obtain this result by appealing to previous work on abstract random evolutions. To set it up, define the operator $\mathbb{A} := \frac{1}{2}(\mathbb{A}_0 + \mathbb{A}_1)$ with domain given by the intersection of the domains of $\mathbb{A}_0$ and $\mathbb{A}_1$. Assume this domain of $\mathbb{A}$ and the range of $\mu - \mathbb{A}$ are both dense in $L^2[0,1]$ for sufficiently large $\mu > 0$. Then Theorem 2.1 of [39] ensures that the closure of $\mathbb{A}$ is the infinitesimal generator of a strongly continuous semigroup $\exp(\mathbb{A}t)$ defined on $L^2[0,1]$, which we assume to be the solution operator of (3.25). Theorem 2.1 of [39] gives the convergence,

$$u(x,t) \to \exp(\mathbb{A}t) u(x,0), \quad \text{in probability as } \alpha \to \infty,$$

where $u(x,t)$ is the solution of (2.4) (defined in (2.6)), for each initial condition $u(x,0) \in L^2[0,1]$.

It is straightforward to solve (3.25). In particular, if $\gamma<4$, then

$$\overline{u}(x,t)=\sum_{k=1}^{\infty}e^{-\lambda_k t}a_k\Big(\sin(\sqrt{\lambda_k}x)+\big(2/\gamma\sqrt{\lambda_k}\sec(\sqrt{\lambda_k})-\tan(\lambda_k)\big)\cos(\sqrt{\lambda_k}x)\Big), \quad (3.26)$$

where $\{\lambda_k\}_{k=1}^{\infty}$ are positive solutions to the transcendental equation

$$\big(\gamma^2/4+\lambda\big)\sin(\sqrt{\lambda})=\gamma\sqrt{\lambda},$$

and $\{a_k\}_{k=1}^{\infty}$ are chosen to satisfy the initial conditions. If $\gamma>4$, then

$$\begin{aligned}\overline{u}(x,t)=&e^{\lambda_0 t}a_0\Big(\sinh(\sqrt{\lambda_k}x)+\big(2/\gamma\sqrt{\lambda_k}\operatorname{sech}(\sqrt{\lambda_k})-\tanh(\lambda_k)\big)\cosh(\sqrt{\lambda_k}x)\Big)\\&+\sum_{k=1}^{\infty}e^{-\lambda_k t}a_k\Big(\sin(\sqrt{\lambda_k}x)+\big(2/\gamma\sqrt{\lambda_k}\sec(\sqrt{\lambda_k})-\tan(\lambda_k)\big)\cos(\sqrt{\lambda_k}x)\Big),\end{aligned} \quad (3.27)$$

where $\{\lambda_k\}_{k=1}^{\infty}$ are as before, but $\lambda_0>0$ is the positive solution to the transcendental equation

$$\big(\gamma^2/4-\lambda\big)\sinh(\sqrt{\lambda})=\gamma\sqrt{\lambda}.$$

Hence, we recover the critical value $\gamma_c^{\mathrm{sw}}=4$ found in Theorem 3.1 in the fast switching limit. Comparisons of $\overline{u}(x,t)$ and stochastic simulations of $u(x,t)$ are shown in Figure 3.2 for $\gamma=3.9<4$ and $\gamma=4.1>4$. From these plots, we see that as α increases, the mean of u approaches $\overline{u}$ and the standard deviation of u vanishes.

4. Moment PDEs and finite switching rates

The analysis in Section 3 allowed us to study (2.4) in the limit of fast switching ($\alpha\gg1$). In this section, we study (2.4) for finite switching rates by analyzing PDEs for its first and second moments.

Define the expectation

$$m_j(x,t):=\mathbb{E}[u(x,t)1_{J(t)=j}],\quad j\in\{0,1\}, \quad (4.1)$$

where $1_{\{A\}}$ denotes the indicator function on an event A. Since

$$\mathbb{E}[u(x,t)]=m_0(x,t)+m_1(x,t),$$

we will study m_0, m_1 in order to study the mean of $u(x,t)$.

Assume that

$$\mathbb{E}\|u(x,t)\|_{\infty}<\infty,\quad \mathbb{E}\|\tfrac{\partial}{\partial x}u(x,t)\|_{\infty}<\infty,\quad t\geq0. \quad (4.2)$$

Then, we can apply Theorem 1 in [41] to obtain that m_0 and m_1 satisfy the following deterministic PDE,

$$\begin{aligned}&\frac{\partial}{\partial t}\begin{pmatrix}m_0\\m_1\end{pmatrix}=\frac{\partial^2}{\partial x^2}\begin{pmatrix}m_0\\m_1\end{pmatrix}+\alpha W\begin{pmatrix}m_0\\m_1\end{pmatrix}\\&\tfrac{\partial}{\partial x}m_0(0,t)=\gamma m_0(1,t),\qquad \tfrac{\partial}{\partial x}m_0(1,t)=0,\\&\tfrac{\partial}{\partial x}m_1(0,t)=0,\qquad \tfrac{\partial}{\partial x}m_1(1,t)=-\gamma m_1(0,t),\end{aligned} \quad (4.3)$$

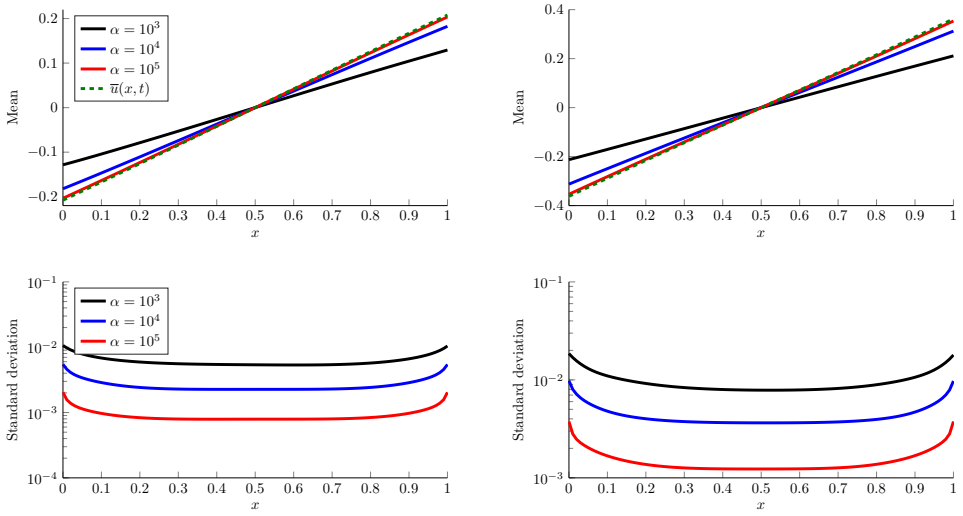

FIG. 3.2. *Random solution becomes deterministic in the limit of fast switching. The top left panel plots the empirical (Monte Carlo) mean (4.26) for* $\gamma = 3.9$, $N = 101$, *at time* $t = 1$ *for* $K = 10^3$ *trials, for various values of the switching rate,* α. *As* α *increases, the empirical mean converges to the solution* $\overline{u}(x,t)$ *of (3.25) given by the dashed green curve. The initial conditions are such that* $a_1 = 1$ *and* $a_k = 0$ *for* $k > 1$ *in (3.26). The bottom left panel plots the corresponding empirical standard deviations. The right two panels are the same, but with* $\gamma = 4.1$, *and the initial conditions are such that* $a_0 = 1$ *and* $a_k = 0$ *for* $k > 0$ *in (3.27).*

where W is the matrix (3.21).

Assuming (4.2), Theorem 1 in [41] guarantees that (4.3) holds. To provide intuition, we note that one can use the method of lines discretization from Section 3 above to quickly rederive (4.3). Suppose $U_N(t)$ is the spatially discretized approximation to $u(x,t)$ satisfying (3.7). Adapting previous analysis of a different random PDE [13], define the spatially discretized analog of (4.1),

$$M_j(t) := \mathbb{E}[U_N(t)1_{J(t)=j}] = \int p_j(\mathbf{u},t)\mathbf{u}\,d\mathbf{u}, \tag{4.4}$$

where $p_j(\mathbf{u},t)$ is the probability density in (3.18). To derive an equation for the time evolution of M_j, multiply both sides of the Chapman-Kolmogorov Equation (3.19) by $\mathbf{u}$ and integrate with respect to $\mathbf{u}$ to obtain

$$\begin{aligned} \tfrac{\partial}{\partial t} M_j &= -\int \nabla\cdot(A_j\mathbf{u}p_j)\mathbf{u}\,d\mathbf{u} + \alpha(M_{1-j} - M_j) \\ &= A_j M_j + \alpha(M_{1-j} - M_j), \quad j = 0,1, \end{aligned} \tag{4.5}$$

where we have integrated by parts and used that $p_j(\mathbf{u},t) \to 0$ as $\|\mathbf{u}\| \to \infty$. Formally retaking the continuum limit $N \to \infty$ then yields (4.3).

4.1. Mean PDE spectral analysis. To analyze (4.3), we introduce the ansatz

$$m_j(x,t) = e^{\lambda t}\varphi_j(x), \tag{4.6}$$

which yields the spectral problem

$$\begin{aligned}
&\lambda\begin{pmatrix}\varphi_0\\ \varphi_1\end{pmatrix}=\frac{d^2}{dx^2}\begin{pmatrix}\varphi_0\\ \varphi_1\end{pmatrix}+\alpha W\begin{pmatrix}\varphi_0\\ \varphi_1\end{pmatrix},\\
&\varphi_0'(0)=\gamma\varphi_0(1), \qquad \varphi_0'(1)=0,\\
&\varphi_1'(0)=0, \qquad \varphi_1'(1)=-\gamma\varphi_1(0).
\end{aligned} \tag{4.7}$$

Changing coordinates by defining

$$\psi_0:=\alpha(\varphi_0+\varphi_1), \quad \psi_1:=\alpha(\varphi_1-\varphi_0), \tag{4.8}$$

we have that (4.7) becomes

$$\frac{d^2}{dx^2}\begin{pmatrix}\psi_0\\ \psi_1\end{pmatrix}=\begin{pmatrix}\lambda & 0\\ 0 & \lambda+2\alpha\end{pmatrix}\begin{pmatrix}\psi_0\\ \psi_1\end{pmatrix}, \tag{4.9}$$

$$\begin{aligned}
&\psi_0'(1)-\psi_1'(1)=0, \qquad \psi_0'(0)-\psi_1'(0)=\gamma\big(\psi_0(1)-\psi_1(1)\big),\\
&\psi_0'(0)+\psi_1'(0)=0, \qquad \psi_0'(1)+\psi_1'(1)=-\gamma\big(\psi_0(0)+\psi_1(0)\big).
\end{aligned} \tag{4.10}$$

Solving (4.9), the eigenfunctions are of the form

$$\begin{aligned}
\psi_0(x)&=a\sinh(\sqrt{\lambda}x)+b\cosh(\sqrt{\lambda}x),\\
\psi_1(x)&=c\sinh(\sqrt{\lambda+2\alpha}x)+d\cosh(\sqrt{\lambda+2\alpha}x).
\end{aligned} \tag{4.11}$$

Plugging these solution forms into (4.10) yields the following system of linear equations for the constants a, b, c, and d,

$$R(a,b,c,d)^T=0, \tag{4.12}$$

where R is the matrix

$$R=\begin{pmatrix}
\sqrt{\lambda} & 0 & \sqrt{\lambda+2\alpha} & 0\\
\sqrt{\lambda}\cosh(\sqrt{\lambda}) & \sqrt{\lambda}\sinh(\sqrt{\lambda}) & -\sqrt{\lambda+2\alpha}\cosh(\sqrt{\lambda+2\alpha}) & -\sqrt{\lambda+2\alpha}\sinh(\sqrt{\lambda+2\alpha})\\
\sqrt{\lambda}\cosh(\sqrt{\lambda}) & \gamma+\sqrt{\lambda}\sinh(\sqrt{\lambda}) & \sqrt{\lambda+2\alpha}\cosh(\sqrt{\lambda+2\alpha}) & \gamma+\sqrt{\lambda+2\alpha}\sinh(\sqrt{\lambda+2\alpha})\\
\gamma\sinh(\sqrt{\lambda})-\sqrt{\lambda} & \gamma\cosh(\sqrt{\lambda}) & -\gamma\sinh(\sqrt{\lambda+2\alpha})+\sqrt{\lambda+2\alpha} & -\gamma\cosh(\sqrt{\lambda+2\alpha})
\end{pmatrix}.$$

Since we seek non-trivial ψ_0 and ψ_1, we need the determinant of R to be zero, which gives the following transcendental equation for λ:

$$f(\lambda)=0, \tag{4.13}$$

where

$$\begin{aligned}
f(\lambda)=&\sinh\big(\sqrt{\lambda}\big)\Big[2\gamma\lambda\sqrt{2\alpha+\lambda}+\sinh\big(\sqrt{2\alpha+\lambda}\big)\big(2\lambda^2+(4\alpha-\gamma^2)\lambda-\gamma^2\alpha\big)\Big]\\
&+\sqrt{\lambda}\gamma^2\sqrt{2\alpha+\lambda}\cosh\big(\sqrt{\lambda}\big)\cosh\big(\sqrt{2\alpha+\lambda}\big)\\
&+\sqrt{\lambda}\gamma\Big[2(2\alpha+\lambda)\sinh\big(\sqrt{2\alpha+\lambda}\big)+\gamma\sqrt{2\alpha+\lambda}\Big].
\end{aligned}$$

We seek conditions on $\alpha>0$ and $\gamma>0$ to ensure that (4.13) has a solution $\lambda\in\mathbb{C}$ with positive real part.

Observe that if $\lambda\in\mathbb{C}$ and $\mathrm{Re}(\lambda)>0$, then λ is a root of $f(\lambda)$ if and only if λ is a root of

$$\mathcal{F}(\lambda):=\frac{f(\lambda)}{(\lambda^2+\lambda+1)\sinh(\sqrt{\lambda})\sinh(\sqrt{2\alpha+\lambda})}. \tag{4.14}$$

Note that $\mathcal{F}$ has a removable singularity at $\lambda=0$, and so we define

$$\mathcal{F}(0)=\lim_{\lambda\to 0}\mathcal{F}(\lambda)=\gamma^2\sqrt{2\alpha}\coth\left(\sqrt{\alpha/2}\right)+\alpha\gamma(4-\gamma)\in\mathbb{R}. \tag{4.15}$$

Further, we have defined $\mathcal{F}$ such that

$$\lim_{|\lambda|\to\infty}\mathcal{F}(\lambda)=2, \quad \text{if } \mathrm{Re}(\lambda)\geq 0. \tag{4.16}$$

Hence, the continuity of $\mathcal{F}$ and the intermediate value theorem imply that if $\mathcal{F}(0)<0$, then $\mathcal{F}$ has at least one strictly positive real root. Rearranging (4.15), we have that $\mathcal{F}$ has a strictly positive real root if $\alpha>0$ and $\gamma>0$ satisfy

$$\gamma>\gamma^*(\alpha):=4\left(1-\sqrt{2/\alpha}\coth\left(\sqrt{\alpha/2}\right)\right)^{-1}>0. \tag{4.17}$$

Further, note that

$$\lim_{\alpha\to\infty}\gamma^*(\alpha)=4, \tag{4.18}$$

which recovers the critical value of γ found in Section 3 in the fast switching limit.

To summarize, if $\gamma>\gamma^*(\alpha)>0$, then our spectral analysis predicts that the mean of $u(x,t)$ grows exponentially in magnitude. We are interested in the case in which $\gamma<\gamma_c\approx 17.8$ so that solutions to the two individual systems ((2.1) and (2.3)) decay to zero, but the mean of the switched system (2.4) grows exponentially in magnitude. Setting $\gamma^*(\alpha)<\gamma_c$ and solving for $\alpha>0$, we find that if α is greater than approximately 4.162 and $\gamma\in(\gamma^*(\alpha),\gamma_c)$, then we obtain such a system. This region of parameter space where the mean of the switched system grows exponentially but the individual systems decay is shown in Figure 4.1.

We note that since the operator involved in (4.3) is not necessarily self-adjoint, we cannot make rigorous statements about the large-time behavior of the mean of $u(x,t)$ for arbitrary initial conditions. However, we can make such statements about certain initial conditions. For example, if $\gamma>\gamma^*(\alpha)>0$, then we have proven above that there exists a positive $\lambda>0$ satisfying (4.13). Hence, there exists nontrivial a,b,c,d satisfying (4.12). Define φ_0,φ_1 by (4.8), where ψ_0,ψ_1 are defined by (4.11) using this choice of $\alpha>0,\lambda>0$ and a,b,c,d. Define the random initial condition,

$$u(x,0)=\begin{cases}2\varphi_0(x) & \text{if } J(0)=0,\\ 2\varphi_1(x) & \text{if } J(0)=1,\end{cases}$$

where J starts in its invariant measure, $\mathbb{P}(J(0)=0)=\mathbb{P}(J(0)=1)=1/2$. It follows that $m_j(x,t):=e^{\lambda t}\varphi_j(x)$ satisfies (4.3), and thus the mean of u is given by

$$\mathbb{E}[u(x,t)]=m_0(x,t)+m_1(x,t)=e^{\lambda t}\alpha^{-1}\left(a\sinh(\sqrt{\lambda}x)+b\cosh(\sqrt{\lambda}x)\right),$$

as long as (4.3) has a unique solution for the initial condition, $m_j(x,0)=\varphi_j(x)$. It follows from (4.10) that if $a=b=0$, then $\psi_1\equiv 0$, and thus a,b,c,d are trivial. Thus, a and b cannot both be zero, and we conclude that the mean grows exponentially for this initial condition.

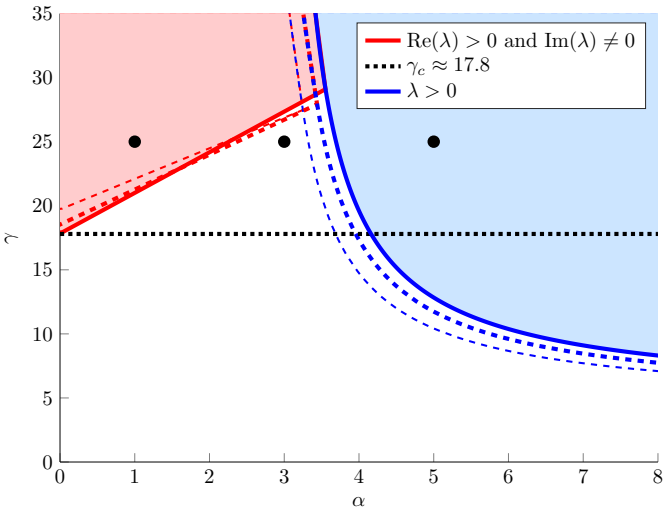

FIG. 4.1. *Phase diagram for* $\mathbb{E}[u(x,t)]$. *If the parameters* (α,γ) *lie in the red (upper left), blue (upper right), or white (lower) regions, then the mean oscillates with ever increasing amplitude, grows exponentially in magnitude, or decays to zero, respectively. The boundary of the blue region is* $\gamma^*(\alpha)$ *in (4.17), and the red region was found numerically from (4.20). The blue and red dashed curves are the boundaries of the corresponding regions for the mean (4.4) of the discretized system (3.7) with* $N=3$ *(thin dashed curves) and* $N=5$ *(thicker dashed curves). The intersection of the red curve with the vertical axis recovers the critical value* $\gamma_c \approx 17.8$ *(dotted black line) found for the non-switching system (2.3) [27, 36]. If* (α,γ) *is above the blue curve, but below the black dotted line, then the mean of the switched system (2.4) grows exponentially in magnitude while the non-switched systems systems (2.1) and (2.3) decay to zero. The three black dots are at* (α,γ) *equal to* $(1,25)$, $(3,25)$, *or* $(5,25)$, *which are the parameters in Figs. 4.2 and 4.3.*

4.1.1. Winding number analysis. So far, we have given a sufficient condition for the existence of an odd number of strictly positive real roots of (4.13). To determine the number of real or complex roots of $\mathcal{F}(\lambda)$ in $\mathrm{Re}(\lambda)>0$ and thereby complete the phase diagram of $\mathbb{E}[u(x,t)]$, we follow [16,26] and use the argument principle of complex analysis.

Specifically, we compute the change in the argument of $\mathcal{F}(\lambda)$ over the contour

$$\Gamma_R \cup \Gamma_+ \cup \Gamma_- \in \mathbb{C},$$

where Γ_R is the semicircle, $|\lambda|=R$ with $\mathrm{Re}(\lambda)>0$, and $\Gamma_\pm = \pm i\lambda_I$ for $\lambda_I \in [0,R]$. Assuming there are no pure imaginary roots of $\mathcal{F}(\lambda)$, the argument principle [1] implies that the number of roots, n, of $\mathcal{F}(\lambda)$ in $\mathrm{Re}(\lambda)>0$ is

$$n = \frac{1}{2\pi}\left(\lim_{R\to\infty} [\arg \mathcal{F}]_{\Gamma_R} + \lim_{R\to\infty} [\arg \mathcal{F}]_{\Gamma_+} + \lim_{R\to\infty} [\arg \mathcal{F}]_{\Gamma_-} \right) + p, \tag{4.19}$$

where $[\arg \mathcal{F}]_\Gamma$ denotes the change in the argument of $\mathcal{F}$ over the contour Γ oriented counterclockwise, and p is the number of poles of $\mathcal{F}(\lambda)$ in $\mathrm{Re}(\lambda)>0$ counted by their multiplicity.

We now analyze (4.19) to determine n. It is easy to see that $p=0$. Further, if $\overline{z}$ denotes the complex conjugate of $z\in\mathbb{C}$, then $\mathcal{F}(\overline{\lambda}) = \overline{\mathcal{F}(\lambda)}$, and thus $[\arg \mathcal{F}]_{\Gamma_+} = [\arg \mathcal{F}]_{\Gamma_-}$. Further, it follows from (4.16) that $\lim_{R\to\infty} [\arg \mathcal{F}]_{\Gamma_R} = 0$. Putting this together, we

have that (4.19) becomes

$$n = \frac{1}{\pi} \lim_{R\to\infty} [\arg \mathcal{F}]_{\Gamma_+}. \tag{4.20}$$

Indeed, it follows from (4.15) and (4.16) that $\lim_{R\to\infty}[\arg\mathcal{F}]_{\Gamma_+}$ must be a multiple of π.

By (4.20), computing the change in the argument of $\mathcal{F}$ (i.e., the winding number) over the contour $\Gamma_+ \subset \mathbb{C}$ yields the number of roots of $\mathcal{F}(\lambda)$ in $\mathrm{Re}(\lambda) > 0$. This is illustrated in Figure 4.2, where we plot in the complex plane the path of $\mathcal{F}(i\lambda_I)$ for λ_I ranging from a large positive value to 0. For one parameter set ($\alpha = 1$ and $\gamma = 25$), the path of $\mathcal{F}$ wraps around the origin once (black curve), so the change in the argument of $\mathcal{F}$ is 2π and thus $\mathcal{F}$ has two roots with positive real part ($n = 2$). To determine if these two roots are real or complex, observe that $\mathcal{F}$ can be written in the form

$$\mathcal{F}(\lambda) = \left(\lambda^2 + \lambda + 1\right)^{-1} \left(h(\lambda) + q(\lambda)\right),$$

where

$$h(\lambda) = \gamma\sqrt{\lambda}\,\mathrm{csch}\left(\sqrt{\lambda}\right)\mathrm{csch}\left(\sqrt{2\alpha+\lambda}\right)\Big[\gamma\sqrt{2\alpha+\lambda} + \gamma\sqrt{2\alpha+\lambda}\cosh\left(\sqrt{\lambda}\right)\cosh\left(\sqrt{2\alpha+\lambda}\right) + 2(2\alpha+\lambda)\sinh\left(\sqrt{2\alpha+\lambda}\right) + 2\sqrt{\lambda}\sqrt{2\alpha+\lambda}\sinh\left(\sqrt{\lambda}\right)\Big],$$

and $q(\lambda)$ is the quadratic

$$q(\lambda) = 2\lambda^2 + (4\alpha - \gamma^2)\lambda - \gamma^2\alpha.$$

Since $h(\lambda) > 0$ if $\lambda > 0$, and $q(\lambda) > 0$ if $\lambda > \lambda_+ > 0$, where

$$\lambda_+ := \frac{\gamma^2 - 4\alpha + \sqrt{(\gamma^2-4\alpha)^2 + 8\gamma^2\alpha}}{4},$$

it follows that any positive real root of $\mathcal{F}$ must lie in the interval $(0, \lambda_+)$. It is straightforward to numerically verify that $\mathcal{F}$ has no positive real roots for $\alpha = 1$ and $\gamma = 25$ by evaluating $\mathcal{F}(\lambda)$ for λ ranging from 0 to λ_+. Hence, the two roots of $\mathcal{F}$ for $\alpha = 1$ and $\gamma = 25$ are complex conjugates, and thus the mean oscillates with ever increasing amplitude.

Keeping $\gamma = 25$ and increasing the switching rate to $\alpha = 3$, we see in Figure 4.2 that the change in the argument of $\mathcal{F}$ is zero (blue curve) and thus $n = 0$. Hence, the mean decays to zero for this parameter choice.

Finally, if we keep $\gamma = 25$ and raise the switching rate to $\alpha = 5$, then $\gamma > \gamma^*(\alpha) > 0$, and therefore there are an odd number of strictly positive real roots of (4.13). Plotting the path of $\mathcal{F}$ in Figure 4.2 (red curve), we see that the change in the argument of $\mathcal{F}$ is π, and thus (4.13) has no complex roots. Therefore, the mean grows exponentially in magnitude for this parameter choice.

Putting this together, if $\gamma = 25$, then the mean oscillates with ever increasing amplitude for slow switching ($\alpha = 1$), decays to zero for intermediate switching ($\alpha = 3$), and grows exponentially in magnitude for fast switching ($\alpha = 5$). These predictions are confirmed by simulations of (4.3) in Figure 4.3.

In Figure 4.1, we use (4.17) and this numerical calculation of the winding number to create a phase diagram of (4.3) indicating the regions of parameter space in which the mean of u either decays, grows exponentially in magnitude, or oscillates with ever

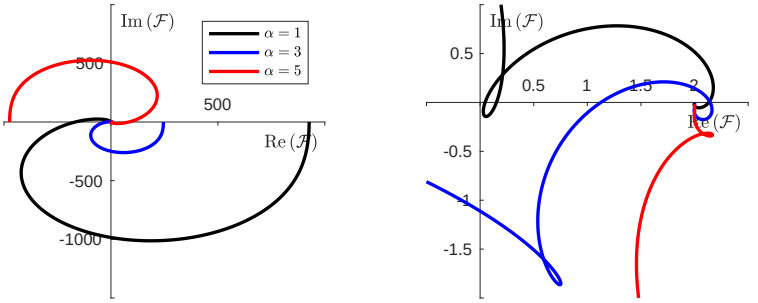

FIG. 4.2. *Path of* $(Re(\mathcal{F}(i\lambda_I)), Im(F(i\lambda_I)))$ *in the complex plane as* λ_I *ranges from* 10^3 *to* 0. *From the left plot, it is not clear what the change in the argument of* $\mathcal{F}$ *is for each curve. Zooming in, the right plot reveals that the changes in the arguments are* 2π *for the black curve,* 0 *for the blue curve, and* π *for the red curve. We set* $\gamma = 25$.

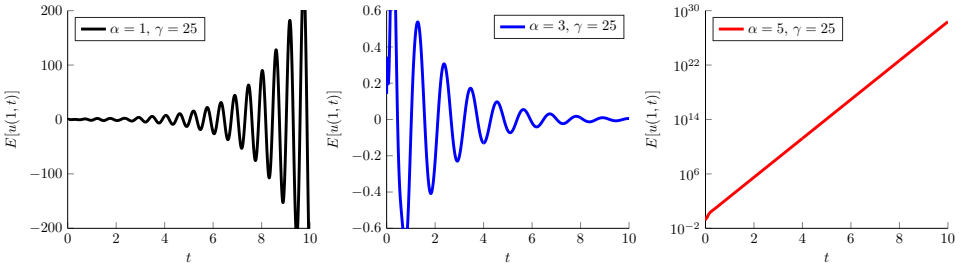

FIG. 4.3. *The mean solution can oscillate with ever increasing amplitude (left plot), decay to zero (middle plot), or grow exponentially (right plot) depending on the switching rate* $\alpha > 0$. *By numerically solving (4.3), we plot the mean* $\mathbb{E}[u(x,t)]$ *evaluated at* $x = 1$ *as a function of time for* $\gamma = 25$ *and either* $\alpha = 1$ *(left plot),* $\alpha = 3$ *(middle plot), or* $\alpha = 5$ *(right plot).*

increasing amplitude. We also plot in Figure 4.1 the phase diagram of the mean (4.4) of the discretized system (3.7) for $N = 3$ and $N = 5$ (dashed curves). That is, since the evolution Equation (4.5) for the discretized mean can be written in the form

$$\frac{d}{dt}\begin{pmatrix} M_0(t) \\ M_1(t) \end{pmatrix} = \begin{pmatrix} A_0 - \alpha I & \alpha I \\ \alpha I & A_1 - \alpha I \end{pmatrix} \begin{pmatrix} M_0(t) \\ M_1(t) \end{pmatrix} \in \mathbb{R}^{2(N+1)},$$

we plot the regions of parameter space in which the block matrix

$$\begin{pmatrix} A_0 - \alpha I & \alpha I \\ \alpha I & A_1 - \alpha I \end{pmatrix} \in \mathbb{R}^{2(N+1)\times 2(N+1)}, \tag{4.21}$$

has a positive eigenvalue or a complex eigenvalue with positive real part. These regions of parameter space for the discretized system (3.7) converge rapidly to the corresponding regions of the PDE (2.4). Indeed, they are close to indistinguishable for $N \geq 10$, so we only show them for $N = 3$ and $N = 5$ in Figure 4.1.

4.2. Two-point correlations. To obtain more detailed information on realizations of (2.4), we now investigate its second moment. Define the two-point correlation

functions,

$$c_j(x,y,t) := \mathbb{E}[u(x,t)u(y,t)1_{J(t)=j}], \quad j \in \{0,1\}.$$

If we again assume (4.2), then we can apply Theorem 1 in [41] to obtain that c_0 and c_1 satisfy the following deterministic PDE on the square $[0,1]^2$,

$$\begin{aligned}
&\frac{\partial}{\partial t}\begin{pmatrix} c_0 \\ c_1 \end{pmatrix} = \frac{\partial^2}{\partial x^2}\begin{pmatrix} c_0 \\ c_1 \end{pmatrix} + \frac{\partial^2}{\partial y^2}\begin{pmatrix} c_0 \\ c_1 \end{pmatrix} + \alpha W \begin{pmatrix} c_0 \\ c_1 \end{pmatrix}, \quad (x,y) \in [0,1]^2, t > 0 \\
&\tfrac{\partial}{\partial x} c_0(0,y,t) = \gamma c_0(1,y,t), \qquad \tfrac{\partial}{\partial x} c_0(1,y,t) = 0, \\
&\tfrac{\partial}{\partial x} c_1(0,y,t) = 0, \qquad \tfrac{\partial}{\partial x} c_1(1,y,t) = -\gamma c_1(0,y,t), \\
&\tfrac{\partial}{\partial y} c_0(x,0,t) = \gamma c_0(x,1,t), \qquad \tfrac{\partial}{\partial y} c_0(x,1,t) = 0, \\
&\tfrac{\partial}{\partial y} c_1(x,0,t) = 0, \qquad \tfrac{\partial}{\partial y} c_1(x,1,t) = -\gamma c_1(x,0,t).
\end{aligned} \tag{4.22}$$

The variance of u as a function of x and t is then given in terms of the solutions to (4.3) and (4.22),

$$\mathrm{Var}(u(x,t)) = \mathbb{E}\Big[\big(u(x,t) - \mathbb{E}[u(x,t)]\big)^2\Big] = c_0(x,x,t) + c_1(x,x,t) - \big(m_0(x,t) + m_1(x,t)\big)^2.$$

We are not able to solve (4.22) analytically. However, one can discretize the two spatial variables x and y in (4.22) and use the method of lines to find a numerical approximation. Equivalently, one can first consider the spatially discretized system (3.7) for $U_N(t) \in \mathbb{R}^{N+1}$, and then derive evolution equations for its two-point correlations. That is, analogous to the evolution Equation (4.5) for the first moments (4.4), the two-point correlations,

$$C_j(t) := \mathbb{E}[U_N(t)(U_N(t))^T 1_{J(t)=j}] \in \mathbb{R}^{(N+1)\times(N+1)}, \quad j \in \{0,1\}, \tag{4.23}$$

evolve according to

$$\tfrac{d}{dt} C_j(t) = A_j C_j(t) + C_j(t) A_j^T + \alpha(C_{1-j}(t) - C_j(t)) \quad j \in \{0,1\}. \tag{4.24}$$

Putting the matrices $C_0(t), C_1(t) \in \mathbb{R}^{(N+1)\times(N+1)}$ into a vector $C(t) \in \mathbb{R}^{2(N+1)^2}$, the evolution Equation (4.24) can be written in the form

$$\tfrac{d}{dt} C(t) = BC(t), \tag{4.25}$$

for a matrix $B \in \mathbb{R}^{2(N+1)^2 \times 2(N+1)^2}$ chosen appropriately.

We can therefore analyze the spectrum of B to determine the asymptotic growth or decay of $C(t)$. In Figure 4.4, we plot the regions of (α,γ) parameter space in which B has a positive eigenvalue or all negative eigenvalues, which yields a phase diagram for $C(t)$. From this plot, we see that there is a region of parameter space in which the mean of $U_N(t)$ decays exponentially, but its second moment (and therefore its variance) grows exponentially.

We note that in the region of Figure 4.4 in which both the mean and the variance of $U_N(t)$ decay to zero (below the green curve), it follows from Chebyshev's inequality that $U_N(t) \to 0$ in probability as $t \to \infty$.

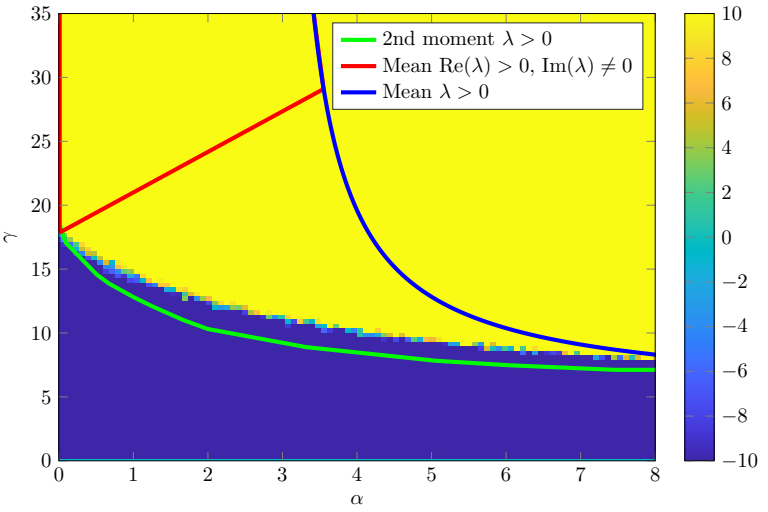

FIG. 4.4. *Comparison of empirical mean with actual mean and variance. Above the green curve, the variance of $U_N(t)$ grows exponentially in time (we take $N=51$). Above the red and blue curves, the mean of $\mathbb{E}[u(x,t)]$ grows in magnitude. The colors of the heat map give the logarithm of the absolute value of a realization of the empirical (Monte Carlo) mean (4.26) with $K=10^2$, $N=51$, and $T=10^2$, where we take this logarithm to be 10 if it is greater than 10 and -10 if it is less than -10. As expected, there is a region of parameter space in which the mean decays in time, but the computed empirical mean is large. This discrepancy is because the variance grows exponentially in this region, and therefore it is not computationally feasible to verify that the empirical mean decays to zero.*

4.3. Stochastic simulations. Finally, we compare our predictions of the mean behavior with empirical means computed from a large number of stochastic realizations of (2.4). That is, for $T>0$ we generate K independent stochastic realizations of the jump process $\{\{J^{(k)}(t)\}_{t=0}^{t=T}\}_{k=1}^{K}$, and then compute the corresponding solution $U_N^{(k)}(T)$ to (3.7) in order to approximate the solution $u^{(k)}(x,T)$ to (2.4). We then compare realizations of the empirical (Monte Carlo) mean,

$$\frac{1}{K}\sum_{k=1}^{K} U_N^{(k)}(T), \tag{4.26}$$

with the actual mean $\mathbb{E}[u(x,t)]$ whose behavior we determined by analyzing (4.3).

In Figure 4.4, we plot realizations of the empirical mean (4.26) as a function of parameters α and γ for $K=10^4$, $N=10$, and $T=10^2$. From this plot, we see that the behavior of the empirical mean agrees with our predictions, except in a portion of the region of parameter space in which the variance grows, but the mean decays (above the green curve but below the red and blue curves). In this region, the actual mean decays exponentially in time, but the computed empirical means can be quite large.

This discrepancy is to be expected and is due to the number of trials $K=10^4$ being too small. Indeed, it follows from elementary probability theory that we can only expect the empirical mean of a random variable to be close to its actual mean if the number of trials is much larger than the variance of the random variable. Hence, it is not computationally feasible to verify that the empirical mean (4.26) converges to the actual mean in this region of parameter space, since one would need to take K exponentially large in time. To illustrate, if $\alpha=3$, $\gamma=20$, and $N=10$, then a quick

numerical computation gives that the dominant eigenvalue of the matrix controlling the mean behavior (4.21) has real part ≈ -1.6, and the dominant eigenvalue of the matrix controlling the second moment in (4.25) is ≈ 13.9. Therefore, to show that at time $T>0$ the empirical mean (4.26) is of order $e^{-1.6T}$, one would have to take the number of trials K to be at least of order $e^{13.9T}$.

Therefore, this highlights the necessity of our mathematical analysis in order to compute the mean since an estimate of the mean through Monte Carlo simulation is computationally intractable. In addition, this underscores that looking only at the mean can be misleading, and higher order moments are often necessary to understand a randomly switching system's qualitative behavior.

5. Switching between unstable BCs can be stable

So far in this paper, we have shown that a PDE that switches between two stable BCs can result in a solution that grows without bound. In this section, we briefly propose and analyze a model that yields the opposite result. Namely, we find a PDE that switches between two unstable BCs but results in a solution that decays to zero. We note that the average system for this example is stable.

Suppose $u(x,t)$ satisfies the heat equation on the interval $(0,1)$ and suppose the BCs randomly switch between

$$\tfrac{\partial}{\partial x}u(0,t)=\gamma_0 u(1,t), \qquad \tfrac{\partial}{\partial x}u(1,t)=0, \tag{5.1}$$

and

$$\tfrac{\partial}{\partial x}u(0,t)=-\gamma_1 u(1,t), \qquad \tfrac{\partial}{\partial x}u(1,t)=0, \tag{5.2}$$

for $\gamma_0>\gamma_1>0$. That is, $u(x,t)$ satisfies the switching BCs

$$\tfrac{\partial}{\partial x}u(0,t)=((1-J(t))\gamma_0-J(t)\gamma_1)u(1,t), \qquad \tfrac{\partial}{\partial x}u(1,t)=0, \tag{5.3}$$

where $J(t)\in\{0,1\}$ is a two-state Markov jump process with jump rate $\alpha>0$.

The heat equation with the BC (5.1) is again the thermostat model, but the BC in (5.2) yields a sort of anti-thermostat model in which a high temperature at $x=1$ causes *more* heating $x=0$. Not surprisingly, solutions with only the BC in (5.2) grow exponentially for all $\gamma_1>0$. Nevertheless, we will show that one can choose $\gamma_0>\gamma_c$ and $\gamma_1>0$ so that solutions to the randomly switching system (5.3) decay to zero, even though solutions to the two individual non-switched systems ((5.1) and (5.2)) grow without bound. As our analysis of (5.3) is similar to our analysis of (2.4), we merely outline the key steps and give the main results.

5.1. Method of lines. As in Section 3, we can study the randomly switching PDE (5.3) by studying the randomly switching linear ODE

$$\tfrac{d}{dt}U_N(t)=B_{J(t)}U_N(t), \tag{5.4}$$

where $B_0,B_1\in\mathbb{R}^{(N+1)\times(N+1)}$ are the matrices

$$B_j=\frac{1}{(\Delta x)^2}\begin{pmatrix} -2 & 2 & & & -((1-j)\gamma_0-j\gamma_1)2\Delta x \\ 1 & -2 & 1 & & \\ & \ddots & \ddots & \ddots & \\ & & 1 & -2 & 1 \\ & & & 2 & -2 \end{pmatrix}, \qquad j\in\{0,1\}.$$

Again, for fast switching ($\alpha \gg 1$) the behavior is determined by the average matrix, $B := \frac{1}{2}(B_0 + B_1)$. Consulting (3.5), we see that B is the matrix one obtains by a method of lines discretization of the thermostat model with parameter $\gamma = \frac{1}{2}(\gamma_0 - \gamma_1)$. Therefore, (5.3) is stable (respectively, unstable) for sufficiently fast switching if $\frac{1}{2}(\gamma_0 - \gamma_1) \in (0, \gamma_c)$ (respectively, $\frac{1}{2}(\gamma_0 - \gamma_1) \notin [0, \gamma_c]$). Therefore, one can choose γ_0 and γ_1 such that the two individual non-switched systems ((5.1) and (5.2)) are unstable, but the switched system (5.3) is stable for sufficiently fast switching (for example, let $\gamma_0 = 20$, $\gamma_1 = 10$).

5.2. First moment. To analyze the mean of (5.3), define $m_j(x,t)$ as in (4.1) and use the same argument as in Section 4 to show that m_0 and m_1 satisfy

$$\begin{aligned} &\frac{\partial}{\partial t}\begin{pmatrix} m_0 \\ m_1 \end{pmatrix} = \frac{\partial^2}{\partial x^2}\begin{pmatrix} m_0 \\ m_1 \end{pmatrix} + \alpha W \begin{pmatrix} m_0 \\ m_1 \end{pmatrix} \\ &\tfrac{\partial}{\partial x} m_0(0,t) = \gamma_0 m_0(1,t), \qquad \tfrac{\partial}{\partial x} m_0(1,t) = 0, \\ &\tfrac{\partial}{\partial x} m_1(0,t) = -\gamma_1 m_1(1,t), \qquad \tfrac{\partial}{\partial x} m_1(1,t) = 0. \end{aligned} \tag{5.5}$$

The ansatz (4.6) yields the spectral problem

$$\begin{aligned} &\lambda\begin{pmatrix} \varphi_0 \\ \varphi_1 \end{pmatrix} = \frac{\partial^2}{\partial x^2}\begin{pmatrix} \varphi_0 \\ \varphi_1 \end{pmatrix} + \alpha W \begin{pmatrix} \varphi_0 \\ \varphi_1 \end{pmatrix} \\ &\varphi_0'(0) = \gamma_0 \varphi_0(1), \qquad \varphi_0'(1) = 0, \\ &\varphi_1'(0) = -\gamma_1 \varphi_1(1), \qquad \varphi_1'(1) = 0. \end{aligned} \tag{5.6}$$

Letting $\psi_0 = \alpha(\varphi_0 + \varphi_1)$ and $\psi_1 = \alpha(\varphi_1 - \varphi_0)$, it follows that

$$\psi_0(x) = a\cosh(\sqrt{\lambda}(x-1)), \qquad \psi_1(x) = b\cosh(\sqrt{\lambda + 2\alpha}(x-1)),$$

where a and b satisfy

$$\begin{aligned} -(\sqrt{\lambda}\sinh(\sqrt{\lambda}) + \gamma_0)a + (\sqrt{\lambda+2\alpha}\sinh(\sqrt{\lambda+2\alpha}) + \gamma_0)b = 0 \\ -(\sqrt{\lambda}\sinh(\sqrt{\lambda}) - \gamma_1)a - (\sqrt{\lambda+2\alpha}\sinh(\sqrt{\lambda+2\alpha}) - \gamma_1)b = 0. \end{aligned}$$

Since we are looking for a nontrivial solution, we need

$$f_2(\lambda) = 0, \tag{5.7}$$

where

$$\begin{aligned} f_2(\lambda) := \sqrt{2\alpha+\lambda}(\gamma_0 - \gamma_1)\sinh\left(\sqrt{2\alpha+\lambda}\right) \\ + \sqrt{\lambda}\sinh\left(\sqrt{\lambda}\right)\left(2\sqrt{2\alpha+\lambda}\sinh\left(\sqrt{2\alpha+\lambda}\right) + \gamma_0 - \gamma_1\right) - 2\gamma_0\gamma_1. \end{aligned}$$

It is easy to see that

$$\lim_{\lambda \to +\infty} f_2(\lambda) = +\infty.$$

Therefore, if $f_2(0) < 0$, then f has at least one strictly positive real root. Rearranging the condition $f_2(0) < 0$, we have that if $\alpha > 0$, $\gamma_0 > 0$, $\gamma_1 > 0$ are such that

$$0 < \gamma_0 < \gamma_0^*(\alpha, \gamma_1) := \left(1/\gamma_1 - \sqrt{2/\alpha}\,\mathrm{csch}(\sqrt{2\alpha})\right)^{-1}, \tag{5.8}$$

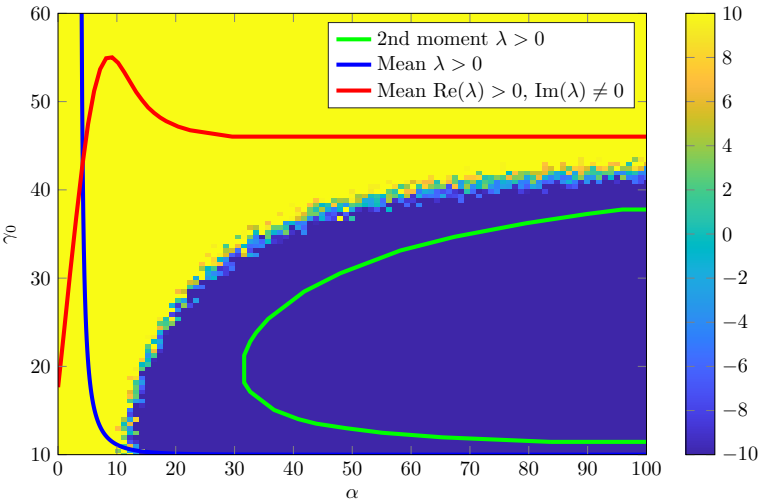

FIG. 5.1. *Phase diagram for the mean of (5.3) and corresponding stochastic simulations. If the parameters (α,γ_0) lie to the left of the blue or red curves, then the mean grows without bound. The blue curve is $\gamma_0^*(\alpha,\gamma_1)$ in (5.8), and the red curve was found numerically from (5.11). To the left of the green curve, the variance of $U_N(t)$ in (5.4) grows exponentially in time (we take $N=21$). The colors of the heat map give the logarithm of the absolute value of a realization of the empirical (Monte Carlo) mean (4.26) of (5.4) with $K=10^2$, $N=21$, and $T=10^2$, where we take this logarithm to be 10 if it is greater than 10 and -10 if it is less than -10. We take $\gamma_1=10$.*

then (5.7) has a positive solution $\lambda>0$. Further, if $\gamma_0>\gamma_1>0$, then $f_2(\lambda)$ is strictly increasing for $\lambda>0$ and thus $f_2(\lambda)$ can have at most one real positive root, and it has such a root if and only if $f_2(0)<0$. We plot $\gamma_0^*(\alpha,\gamma_1)$ in Figure 5.1 (blue curve) for $\gamma_1=10$.

To analyze the roots of $f_2(\lambda)$ in $\mathrm{Re}(\lambda)>0$ in more detail, we use the argument principle of complex analysis as in Section 4. Observe that if $\lambda\in\mathbb{C}$ and $\mathrm{Re}(\lambda)>0$, then λ is a root of $f_2(\lambda)$ if and only if λ is a root of

$$\mathcal{F}_2(\lambda) := \frac{f_2(\lambda)}{(\lambda+1)e^{\sqrt{\lambda}+\sqrt{2\alpha+\lambda}}}. \tag{5.9}$$

Defining the contour $\Gamma_R\cup\Gamma_+\cup\Gamma_-$ as in Section 4.1.1 and assuming there are no pure imaginary roots of $\mathcal{F}_2$, the argument principle implies that the number of roots, n, of $\mathcal{F}_2(\lambda)$ in $\mathrm{Re}(\lambda)>0$ is

$$n=\frac{1}{2\pi}\Big(\lim_{R\to\infty}[\arg\mathcal{F}_2]_{\Gamma_R}+\lim_{R\to\infty}[\arg\mathcal{F}_2]_{\Gamma_+}+\lim_{R\to\infty}[\arg\mathcal{F}_2]_{\Gamma_-}\Big)+p, \tag{5.10}$$

where $[\arg\mathcal{F}_2]_\Gamma$ and p are as in Section 4.1.1.

It is easy to see that $p=0$. Further, $\mathcal{F}_2(\overline{\lambda})=\overline{\mathcal{F}_2(\lambda)}$, and thus $[\arg\mathcal{F}_2]_{\Gamma_+}=[\arg\mathcal{F}_2]_{\Gamma_-}$. Next, we have defined $\mathcal{F}_2$ in (5.9) such that

$$\lim_{|\lambda|\to\infty}\mathcal{F}_2(\lambda)=\frac{1}{2},\quad \text{if } \mathrm{Re}(\lambda)\geq 0.$$

Therefore, $\lim_{R\to\infty}[\arg\mathcal{F}_2]_{\Gamma_R}=0$. Putting this together, we have that (4.19) becomes

$$n=\frac{1}{\pi}\Big(\lim_{R\to\infty}[\arg\mathcal{F}_2]_{\Gamma_+}\Big) \tag{5.11}$$

Equation (5.11) can be calculated numerically from (5.9). Using this method, we give the phase diagram of the mean of (5.3) in Figure 5.1. Specifically, if (α,γ_0) lie to the left of the red curve in Figure 5.1, then (5.7) has imaginary roots with positive real part.

5.3. Second moment. Defining the two-point correlations, $C_0(t),C_1(t)$, of (5.4) as in (4.23), it follows that they evolve according to (4.24) with B_j replacing A_j. Analyzing the spectrum of the linear operator associated with this equation yields the phase diagram for the two-point correlations shown in Figure 5.1. Specifically, if (α,γ_0) lie to the left of the green curve in Figure 5.1, then $C_0(t)$ and $C_1(t)$ grow exponentially in time.

5.4. Stochastic simulations. In Figure 4.4, we plot realizations of the empirical mean (4.26) of (5.4) as a function of parameters α and γ_0 for $K=10^4$, $N=10$ $\gamma_1=10$, and $T=10^2$. From this plot, we see that the behavior of the empirical mean agrees with our predictions, except in a portion of the region of parameter space in which the variance grows, but the mean decays (to the left of the green curve but to the right of the red and blue curves). In this region, the actual mean decays exponentially in time, but the computed empirical means can be large. As in Section 4.3, this discrepancy is to be expected and is due to the number of trials $K=10^4$ being too small.

6. Discussion

In addition to being used in diverse applications [6, 12, 20, 31, 47, 52, 57], recent work has shown that switching systems offer mathematicians novel dynamical behavior and fresh analytical challenges [48]. The present work bolsters this thesis. Using a variety of mathematical methods, we have analyzed a PDE with randomly switching boundary conditions. Our analysis has revealed surprising properties, including that one can choose parameters so that both individual PDE systems are stable, but the switched system is unstable (and vice versa). Our work is related to [8], wherein the authors established qualitatively similar results for randomly switching planar ODEs (see also [10, 40, 44, 49]).

In the context of dynamic networks, a related work is [35], wherein the authors show that synchronous solutions can be stable in certain switching networks for fast switching, even when synchronization is unstable for the individual networks. Further, they show that synchronization can be stable for intermediate switching rates, even with it is unstable for fast switching (see [44] for work on intermediate switching for linear ODEs). We also highlight reference [5], in which the authors bound the probability that a switching system deviates from an average system.

Finally, we emphasize that previous work on switching systems has tended to focus on switching ODEs, in contrast to the switching PDEs studied here. PDEs with randomly switching boundary conditions were first considered in [45]. In that work, the authors assumed a certain contractivity of their systems to prove existence and uniqueness of an invariant measure and to study that measure. The PDE systems in our present work do not fit into this framework, and hence we have devised alternative methods of analysis. We hope that some of the techniques presented here will both inform and be used in future studies of switching PDEs.

Acknowledgement. The author gratefully acknowledges many helpful conversations with Michael J. Ward. The author was supported by NSF grant DMS-RTG 1148230.

REFERENCES

[1] M.J. Ablowitz and A.S. Fokas, *Complex Variables: Introduction and Applications*, Cambridge University Press, 2003.

[2] Y. Bakhtin and T. Hurth, *Invariant densities for dynamical systems with random switching*, Nonlinearity, 25:2937–2952, 2012.

[3] Y. Bakhtin, T. Hurth, S.D. Lawley, and J.C. Mattingly, *Smooth invariant densities for random switching on the torus*, Nonlinearity, 31(4):1331–1350, 2018.

[4] Y. Bakhtin, T. Hurth, and J.C. Mattingly, *Regularity of invariant densities for 1d systems with random switching*, Nonlinearity, 28:3755–3787, 2015.

[5] I. Belykh, V. Belykh, R. Jeter, and M. Hasler, *Multistable randomly switching oscillators: The odds of meeting a ghost*, The European Physical Journal Special Topics, 222:2497–2507, 2013.

[6] I. Bena, *Dichotomous Markov noise: Exact results for out-of-equilibrium systems*, Int. J. Mod. Phys. B, 20:2825–2888, 2006.

[7] M. Benaïm, S. Leborgne, F. Malrieu, and P.A. Zitt, *Quantitative ergodicity for some switched dynamical systems*, Electron. Commun. Probab., 17, 2012.

[8] M. Benaïm, S. Leborgne, F. Malrieu, and P.A. Zitt, *On the stability of planar randomly switched systems*, Ann. Appl. Probab., 24:292–311, 2014.

[9] M. Benaïm, S. Leborgne, F. Malrieu, and P.A. Zitt, *Qualitative properties of certain piecewise deterministic markov processes*, Ann. Inst. H. Poincaré Probab. Statist., 51:1040–1075, 2015.

[10] M. Benaïm and C. Lobry, *Lotka–volterra with randomly fluctuating environments or 'how switching between beneficial environments can make survival harder'*, Ann. Appl. Probab., 26:3754–3785, 2016.

[11] P.C. Bressloff, *Stochastic Processes in Cell Biology*, Springer, 41, 2014.

[12] P.C. Bressloff, *Stochastic switching in biology: from genotype to phenotype*, J. Phys. A, 50(13):133001, 2017.

[13] P.C. Bressloff and S.D. Lawley, *Moment equations for a piecewise deterministic PDE*, J. Phys. A, 48(10):105001, 2015.

[14] P.C. Bressloff and S.D. Lawley, *Stochastically gated diffusion-limited reactions for a small target in a bounded domain*, Phys. Rev. E., 92:062117, 2015.

[15] P.C. Bressloff and S.D. Lawley, *Diffusion on a tree with stochastically gated nodes*, J. Phys. A, 49(24):245601, 2016.

[16] P.C. Bressloff and S.D. Lawley, *Dynamically active compartments coupled by a stochastically gated gap junction*, J. Nonlinear Sci., 27(5):1487?C1512, 2017.

[17] W.L. Briggs, V.E. Henson, and S.F. McCormick, *A multigrid tutorial*, SIAM, 2000.

[18] J. Buceta, K. Lindenberg, and J.M.R. Parrondo, *Spatial patterns induced by random switching*, Fluct. Noise Lett., 2:L21–L29, 2002.

[19] F. Cianciaruso, G. Infante, and P. Pietramala, *Solutions of perturbed Hammerstein integral equations with applications*, Nonlinear Anal. Real World Appl., 33:317–347, 2017.

[20] B. Cloez, R. Dessalles, A. Genadot, F. Malrieu, A. Marguet, and R. Yvinec, *Probabilistic and piecewise deterministic models in biology*, arXiv preprint arXiv:1706.09163, 2017.

[21] B. Cloez and M. Hairer, *Exponential ergodicity for Markov processes with random switching*, Bernoulli, 21(1):505–536, 2015.

[22] A. Faggionato, D. Gabrielli, and M.R. Crivellari, *Non-equilibrium thermodynamics of piecewise deterministic Markov processes*, J. Stat. Phys., 137(2):259?C-304, 2009.

[23] D. Franco, G. Infante, and J. Perán, *A new criterion for the existence of multiple solutions in cones*, Proc. Roy. Soc. Edinburgh Sect. A, 142(5):1043–1050, 2012.

[24] C. Gardiner, *Stochastic Methods*, Springer, 2010.

[25] R. Goebel, J.P. Hespanha, A.R. Teel, C. Cai, and R. Sanfelice, *Hybrid systems: generalized solutions and robust stability*, IFAC Symposium on Nonliear Control Systems, 2004.

[26] J. Gou, W. Chiang, P. Lai, M.J. Ward, and Y. Li, *A theory of synchrony by coupling through a diffusive chemical signal*, Phys. D, 339:1–17, 2017.

[27] P. Guidotti and S. Merino, *Hopf bifurcation in a scalar reaction diffusion equation*, J. Diff. Eqs., 140:209–222, 1997.

[28] P. Guidotti and S. Merino, *Gradual loss of positivity and hidden invariant cones in a scalar heat equation*, Differential Integral Equations, 13:1551–1568, 2000.

[29] M. Hasler, V. Belykh, and I. Belykh, *Dynamics of stochastically blinking systems. Part I: Finite time properties*, SIAM J. Appl. Dyn. Syst., 12(2):1007–1030, 2013.

[30] M. Hasler, V. Belykh, and I. Belykh, *Dynamics of stochastically blinking systems. Part II: Asymptotic properties*, SIAM J. Appl. Dyn. Syst., 12(2):1031–1084, 2013.

[31] J.P. Hespanha, *Modeling and analysis of networked control systems using stochastic hybrid systems*, IFAC Annual Reviews in Control, 38(2):155–170, 2014.

[32] G. Infante, *Nonlocal boundary value problems with two nonlinear boundary conditions*, Commun. Appl. Anal., 12:279–288, 2008.
[33] G. Infante and J.R.L. Webb, *Loss of positivity in a nonlinear scalar heat equation*, NoDEA Nonlinear Diff. Eqs. Appl., 13(2):249–261, 2006.
[34] G. Infante and J.R.L. Webb, *Nonlinear non-local boundary-value problems and perturbed Hammerstein integral equations*, Proc. Edinburgh Math. Soc., 49(2):637–656, 2006.
[35] R. Jeter and I. Belykh, *Synchronization in on-off stochastic networks: windows of opportunity*, IEEE Transactions on Circuits and Systems I: Regular Papers, 62:1260–1269, 2015.
[36] G. Kalna and S. McKee, *The thermostat problem*, TEMA Tend. Mat. Apl. Comput., 3(1):15?C-29, 2002.
[37] G. Kalna and S. McKee, *The thermostat problem with a nonlocal nonlinear boundary condition*, IMA J. Appl. Math., 69(5):437–462, 2004.
[38] I. Karatsompanis and P. K. Palamides, *Polynomial approximation to a non-local boundary value problem*, Comput. Math. Appl., 60(12):3058–3071, 2010.
[39] T. Kurtz, *A random Trotter product formula*, Proc. Amer. Math. Soc., 35:147?C-154, 1972.
[40] G. Lagasquie, *A note on simple randomly switched linear systems*, arXiv preprint, arXiv:1612.01861, 2016.
[41] S.D. Lawley, *Boundary value problems for statistics of diffusion in a randomly switching environment: PDE and SDE perspectives*, SIAM J. Appl. Dyn. Syst., 15:1410–1433, 2016.
[42] S.D. Lawley, *A probabilistic analysis of volume transmission in the brain*, SIAM J. Appl. Math., 78(2):942?C-962, 2018.
[43] S.D. Lawley, J. Best, and M.C. Reed, *Neurotransmitter concentrations in the presence of neural switching in one dimension*, Discrete Contin. Dyn. Syst. Ser. B, 21(7):2255–2273, 2016.
[44] S.D. Lawley, J.C. Mattingly, and M.C. Reed, *Sensitivity to switching rates in stochastically switched ODEs*, Commun. Math. Sci., 12(7):1343–1352, 2014.
[45] S.D. Lawley, J.C. Mattingly, and M.C. Reed, *Stochastic switching in infinite dimensions with applications to random parabolic PDE*, SIAM J. Math. Anal., 47(4):3035–3063, 2015.
[46] R.J. LeVeque, *Finite difference methods for ordinary and partial differential equations: steady-state and time-dependent problems*, SIAM, 2007.
[47] Y.T. Lin and C.R. Doering, *Gene expression dynamics with stochastic bursts: construction and exact results for a coarse-grained model*, Phys. Rev. E, 93:022409, 2016.
[48] F. Malrieu, *Some simple but challenging Markov processes*, arXiv preprint, arXiv:1412.7516, 2014.
[49] F. Malrieu and P.A. Zitt, *On the persistence regime for lotka-Volterra in randomly fluctuating environments*, arXiv preprint arXiv:1601.08151, 2016.
[50] J.J. Nieto and J. Pimentel, *Positive solutions of a fractional thermostat model*, Bound. Value Probl., 5, 2013.
[51] P.K. Palamides, G. Infante, and P. Pietramala, *Nontrivial solutions of a nonlinear heat flow problem via sperner's lemma*, Appl. Math. Lett., 22(9):1444–1450, 2009.
[52] R. Rudnicki and M. Tyran-Kamińska, *Piecewise Deterministic Processes in Biological Models*, Springer, 2017.
[53] A.R. Teel and J.P. Hespanha, *Stochastic hybrid systems: A modeling and stability theory tutorial*, 54th IEEE Conference on Decision and Control (CDC), 2015.
[54] J.R.L. Webb, *Multiple positive solutions of some nonlinear heat flow problems*, Discrete Contin. Dyn. Syst, 895–903, 2005.
[55] J.R.L. Webb, *Optimal constants in a nonlocal boundary value problem*, Nonlinear Anal., 63(5-7):672–685, 2005.
[56] J.R.L. Webb, *Existence of positive solutions for a thermostat model*, Nonlinear Anal. Real World Appl., 13:923–938, 2012.
[57] G. Yin and C. Zhu, *Hybrid Switching Diffusions: Properties and Applications*, Springer New York, 63, 2010.